J. Mol. Biol. (1995) **245**, 508–521

JMB

Dimerization Kinetics of HIV-1 and HIV-2 Reverse Transcriptase: A Two Step Process

Gilles Divita[1]*, Katrin Rittinger[1], Christophe Geourjon[2] Gilbert Deléage[2] and Roger S. Goody[3]

[1]*Max-Planck-Institut für Medizinische Forschung Abteilung Biophysik Jahnstrasse 29, 69120 Heidelberg, Germany*

[2]*Institut de Chimie et Biologie des Protéines, 7 passage du Vercors, 69367 Lyon cedex 07 France*

[3]*Max-Planck-Institut für Molekulare Physiologie Postfach 102664, 44026 Dortmund, Germany*

**Corresponding author*

The dimerization processes of the human immunodeficiency virus (HIV) types 1 and 2 reverse transcriptase (RTs) from their subunits have been investigated using a number of complementary approaches (fluorescence spectroscopy, size exclusion-HPLC and polymerase activity assay). The formation of the native heterodimeric form of HIV-1 and HIV-2 RT occurs in a two step process. The first step is a concentration-dependent association of the two subunits (p66 and p51) to give a heterodimeric intermediate, which slowly isomerizes to the ''mature'' heterodimeric form of the enzyme. For both RTs, the first step behaves as a second order reaction with similar association rate constants (in the range of 2×10^4 to 4×10^4 M^{-1} s^{-1}). This initial dimerization results in a 25% quenching of the intrinsic fluorescence and a 30% decrease in the accessibility of the tryptophan hydrophobic cluster to solvent as revealed by iodide quenching experiments and by monitoring the binding of 1-anilino-8-naphthalenesulphonate. The formation of the intermediate-RT form appears to involve hydrophobic regions of the subunits containing tryptophan residues. This intermediate form is devoid of polymerase activity, but is able to bind primer / template with high affinity. The final stage of the mature RT-heterodimer formation occurs in a slow first order reaction, which is 12-fold faster for HIV-2 (1.2 h^{-1}) than HIV-1 RT (0.1 h^{-1}). At micromolar concentrations, this slow isomerization constitutes the rate limiting step of the RT maturation and the structural change involved appears to be partly associated with the catalytic site, as shown using fluorescent labelled primer / template. On the basis of both the presently available X-ray structure of the HIV-1 RT and the predicted structure of HIV-2 RT, the thumb subdomain of the p51 subunit seems to be involved in this maturation step, which is probably the interaction of this domain with the RNAse H domain of the large subunit. The placement of the fingers subdomain of p51 in the palm subdomain of the p66 subunit may also be associated with formation of mature heterodimeric RTs.

Keywords: Reverse transcriptase; protein folding; fluorescence; dimerization kinetic; HIV

Introduction

Reverse transcriptase (RT) plays a key role in the life cycle of the human immunodeficiency virus (HIV), the etiologic agent of AIDS (Barré-Sinoussi *et al*., 1983; Popovic *et al*., 1984), by converting the single-stranded genomic RNA into double-stranded proviral DNA. HIV-1 RT consists of two subunits, p66 and p51, with molecular weights of 66 kDa and 51 kDa, respectively. The p51 subunit arises by proteolytic cleavage of the p66 subunit by the retroviral protease (Di Marzo-Veronese *et al*., 1986; Lightfoote *et al*., 1986). The two subunits form a stable heterodimer, which constitutes the biologically relevant form of RT (Lowe *et al*., 1988; Müller *et al*., 1989, 1991*a*). HIV-2 RT shows a similar heterodimeric organization with subunit molecular weights of 68 kDa and 54 kDa, respectively. For both HIV-1 and HIV-2 RT, it is clearly established that the heterodimer is the most stable form and that dimerization is absolutely required for all enzymatic

Abbreviations used: HIV-1, HIV-2, human immunodeficiency virus types 1 and 2; RT, reverse transcriptase; p51, etc., 51 kDa protein, etc.; PBS, primer binding site; SOPM, self optimised prediction method; ANS, 1-anilino-8-naphthalenesulphonate; bis-ANS, 8,8'-bis(phenylamino)-5,5'-bi(naphthalene)-1,1'-disulphonate; TEAA, triethylammonium acetate.

0022–2836 / 95 / 050508–14 $08.00 / 0

© 1995 Academic Press Limited

activities (Müller *et al*., 1991*a*; Restle *et al*., 1990, 1992*a*). The recent determination by X-ray crystallography of the three-dimensional structure of HIV-1 RT complexed with a non-nucleoside inhibitor (Kohlstaedt *et al*., 1992) or as a ternary complex with a 19/18 ds DNA template/primer and a monoclonal antibody Fab-fragment (Jacobo-Molina *et al*., 1993) reveals an asymmetric structural organization of the heterodimer p66/p51. The p66 subunit consists of five distinct subdomains, the RNase H subdomain and four subdomains forming the polymerase domain, termed fingers, palm, thumb and connection, according to the nomenclature of Kohlstaedt *et al.* (1992). The p51 subunit contains the four subdomains of the polymerase domain, whose individual structures are similar to those of the corresponding domains of p66, but their relative orientation with respect to one another is significantly different (Kohlstaedt *et al*., 1992; Jacobo-Molina *et al*., 1993). The dimer interface is highly hydrophobic and mainly formed by the interaction between the two connection subdomains (for a review see Nanni *et al*., 1993).

RT is one of the main targets for chemotherapy against HIV. Inhibitors that have been developed mainly interfere with the RT polymerase activity during HIV replication (for reviews see De Clercq, 1992; Grob *et al*., 1992). Recently we have suggested that the dimerization process of RT could provide an additional interesting target for AIDS-chemotherapy (Restle *et al*., 1990; Divita *et al*., 1993*a*). A new class of inhibitors was proposed, which are based on peptides derived from the connection domain as inhibitors of the dimerization process of RT (Divita *et al*., 1994). Although it is clear that the dimeric form is required for all catalytic properties of RT, the process of dimerization and the physical parameters involved in the protein–protein interaction are still not fully understood.

Investigation of the pathway by which the subunits fold and associate is a key approach for a better understanding of the biological structure and function of RT. In most cases, protein association results in successive intermediates that are partially ordered (for a review see Jaenicke, 1987). The process can be characterized in terms of the kinetic, structural and thermodynamic properties of these transient forms. In the work presented here, we have used a number of complementary approaches, including extrinsic and intrinsic fluorescence, size-exclusion HPLC and a polymerase activity assay to understand the molecular process of HIV-1 and HIV-2 RT dimerization and maturation. Trp-fluorescence is usually very sensitive to conformational changes of a protein (for reviews see Eftink, 1991, 1994). RT offers the advantage of containing a large number of Trp residues (37 and 35 residues in HIV-1 and HIV-2 RT, respectively), which are located in part in the substrate binding site (Divita *et al*., 1993*b*) and in part in the connection subdomains involved in the dimerization process (Divita *et al*., 1993*a*). Important information on the variation in the close environment and on the solvent accessibility of Trp residues can be obtained by fluorescence quenching studies (Dobson *et al*., 1994). We have also used an extrinsic fluorescence probe, ANS, which is a monitor of the accessibility of hydrophobic regions of the proteins during the refolding and the dimerization process (Ptitsyn *et al*., 1990). In addition, the binding of a fluorescently labelled primer/template to RT during the dimerization process offers the possibility of obtaining information on the close environment of the catalytic site (Müller *et al*., 1991*b*; Divita *et al*., 1993*b*). The final stage of the heterodimer formation can be directly followed by monitoring the polymerase activity.

Combining these different methods our results indicate that the formation of the mature heterodimeric form of HIV-1 and HIV-2 RT is at least a two step process, which involves first the association of the two subunits by the interaction of the two connection subdomains and thereafter a slow isomerization to give the active form of RT.

Results

RT-dimerization as monitored by intrinsic fluorescence

As previously described, RT-dissociation induced by acetonitrile results in a 25% increase in the intrinsic fluorescence and a 7 nm red shift of the emission spectrum (Divita *et al*., 1993*a*). The large change in fluorescence is a useful tool to monitor the kinetics of monomer association. RTs from HIV-1 and HIV-2 were first dissociated using 20% acetonitrile and the dimerization process was initiated by a 12-fold dilution in acetonitrile-free buffer (pH 8.0). The standard experiments were performed with a final RT concentration of 0.45 μM, at 25°C, in the presence of 5 mM $MgCl_2$. The kinetics of dimerization were followed by measuring the change in the intrinsic fluorescence at 340 nm (excitation at 290 nm).

The kinetics of RT association as monitored by intrinsic fluorescence are shown in Figure 1. The dimerization induced a fluorescence quenching of 20 to 25% and a 6–7 nm blue shift of the emission spectrum, which corresponds to the value expected from the equilibrium dissociation studies. In all cases, the time curves obtained are monophasic and can be fitted in terms of a second order reaction (Table 1). Under the standard conditions, the dimerization process is 1.5-fold faster for HIV-2 RT and the association rate constants (k_{ass}) were $4.1 \times 10^4\ M^{-1}\ s^{-1}$ for HIV-2 and $2.8 \times 10^4\ M^{-1}\ s^{-1}$ for HIV-1, respectively. The half life for the association reaction is dependent on the RT concentration used, as expected for a second order reaction. Under standard conditions, values of 5.1 minutes for HIV-1 and 3.5 minutes for HIV-2 were obtained. At a RT concentration of 1 μM, these values are significantly decreased to 3.1 minutes and 2.4 minutes for HIV-1 and HIV-2, respectively. Thus, there appears to be an approximately linear inverse

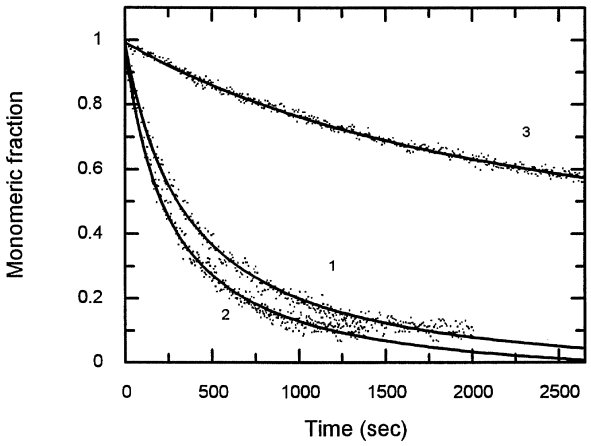

Figure 1. Kinetics of HIV-1 and HIV-2 RT dimerization monitored by intrinsic fluorescence. RTs was first dissociated using 20% acetonitrile and the dimerization was initiated by a 12-fold dilution in an acetonitrile-free buffer, containing 50 mM Tris-HCl (pH 8.0), 5 mM $MgCl_2$, 50 mM KCl, 1 mM dithiothreitol and 10% glycerol. The experiments were performed with a RT concentration of 0.45 μM at 25°C in the presence of 5 mM $MgCl_2$ (HIV-1 RT curve 1 and HIV-2 RT curve 2) or in the absence of $MgCl_2$ for HIV-2 (curve 3). Excitation was performed at 290 nm and Trp-fluorescence was recorded at 340 nm. The data were transformed and expressed in terms of the monomeric fraction using equation (3) and fitted as a second order reaction.

relationship between the half life and the concentration, as expected for the special case of a second order reaction with equal concentrations of reactants, and assuming that only the second order association step is monitored by the fluorescence signal.

The dimerization process of both RTs is dependent on the presence of $MgCl_2$, the association rate constants being reduced 25-fold for HIV-1 RT and 44-fold for HIV-2 RT in the absence of $MgCl_2$. The dimerization process is also strongly dependent on the temperature; at 10°C, the association rate constants are reduced by a factor of 33 (HIV-1) and 53 (HIV-2).

In both cases, the presence of primer/template substrates (18/36-mer) in the association buffer increases the rate of dimerization (twofold (HIV-1) and threefold (HIV-2)). This increase in the rate of dimerization may be correlated with the high thermodynamic stability of the RT–P/T complex, as observed in equilibrium studies (Divita *et al*., 1993*a*).

Dimerization monitored by size exclusion-HPLC

The heterodimeric and monomeric forms of both HIV-1 and HIV-2 RTs can be separated using size exclusion-HPLC (Restle *et al*., 1990). After different times of incubation in an acetonitrile-free buffer the residual monomeric fraction was estimated using size exclusion-HPLC (data not shown). It was observed that after one hour, both RTs are fully dimeric but in contrast, after 30 minutes, which is the lower time limit of this method, HIV-2 RT is completely dimeric whereas only 80% of HIV-1 RT is in the dimeric form. These results are in good agreement with the data obtained by following the intrinsic fluorescence of RTs, which suggested that at the protein concentrations used, the monomer association is achieved after less than one hour at 25°C under standard conditions.

Active RT dimer formation as monitored by polymerase activity

The polymerase and RNAse H activities of both RTs are only expressed in the dimeric form, and the monomers (p51 and p66) are devoid of enzymatic activity (Restle *et al*., 1990, 1992*a*). The formation of active RT was monitored in a time-dependent manner using the polymerase activity assay. RT dissociation was accomplished as described in Materials and Methods and the dimerization reaction was started by 12-fold dilution. The polymerase activity was measured on a sample fraction containing 50 ng of protein at defined time intervals, starting immediately after the dilution. As shown in Figure 2, the kinetics of formation of the active form of HIV-1 and HIV-2 RT were monophasic processes. The kinetics are 12-fold faster for HIV-2 than for HIV-1. In both cases, the rate of formation is

Table 1

HIV-1 and HIV-2 dimerization parameters as monitored by using intrinsic fluorescence

Buffers	HIV-1 RT k_{ass} (M^{-1} s^{-1})	HIV-2 RT k_{ass} (M^{-1} s^{-1})
Standard conditions	$2.8\ 10^4$	$4.1\ 10^4$
At 10°C	$7.4\ 10^2$	$1.05\ 10^3$
Without $MgCl_2$ (EDTA 1 mM)	$9.8\ 10^2$	$8.9\ 10^2$
+Primer/template (1 μM)	$5.4\ 10^4$	$1.34\ 10^5$

Heterodimeric RTs were dissociated using 20% acetonitrile and the dimerization was initiated by a 12-fold dilution in an acetonitrile-free buffer. The kinetics of monomer association were followed by monitoring the intrinsic fluorescence at 340 nm upon excitation at 290 nm at 25°C. In the standard conditions a RT concentration of 0.45 μM was used in the presence of 5 mM $MgCl_2$. The curves were fitted according to a second order reaction with k_{ass} as the second order rate constant.

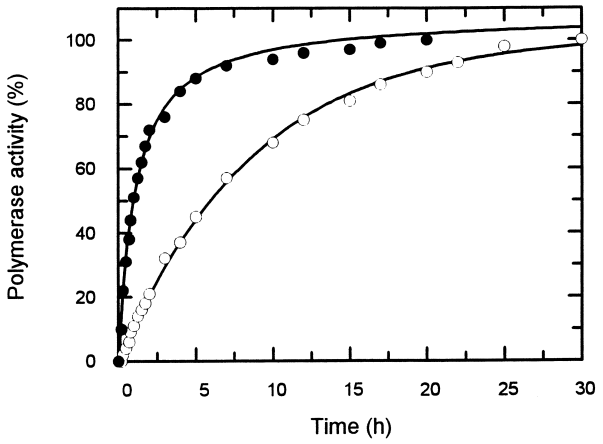

Figure 2. Kinetics of formation of active heterodimeric RT. After different re-association times at 25°C, the HIV-1 (○) and HIV-2 (●) RT polymerase activities were assayed at 37°C as described in Materials and Methods. The enzyme concentration used was 0.45 μM and the curves were fitted according to a single exponential reaction.

not significantly dependent on the RT concentration in the range of 0.2 to 1 μM and can be well fitted with an exponential function. In the lower time limit of the assay method used ($\sim$10 minutes), no lag phase was observed, even at low concentrations. The data were analysed as mono-exponential reactions and the rate constants obtained were 0.12 h^{-1} and 1.6 h^{-1} for HIV-1 and HIV-2 RT, respectively.

These results suggest that the active form of dimeric RT is not immediately formed during initial monomer association, which is finished after one hour as observed by intrinsic fluorescence or HPLC. There must be a second step that takes place after the initial association.

Simulation of the HIV-2 RT dimerization kinetic using the program KinSim showed that for a two step mechanism, with the rate constants of 4.1×10^4 M^{-1} s^{-1} for k_1 and 1.6 h^{-1} for k_2, a lag phase in the polymerase assay kinetics should be observed at dimerization times of less than six minutes. This is in the range of the dead time of the activity assay used, which is the explanation for the absence of the lag phase.

RT-dimerization followed by extrinsic ANS-fluorescence

ANS can be used as a probe for monitoring the variation in the exposure of the hydrophobic regions of a protein and can be used to detect intermediates in protein folding and association (Ptitsyn *et al*., 1990; Ptitsyn, 1994). The binding of ANS or bis-ANS to dissociated RT results in a large increase in the fluorescence of the probe, 10 and 15-fold for ANS and bis-ANS, respectively, and a 45 nm blue shift of the emission spectrum from 540 nm to 495 nm (data not shown). Both are due to non-covalent interactions of ANS or bis-ANS with exposed hydrophobic surfaces on the protein. The change in ANS-fluorescence

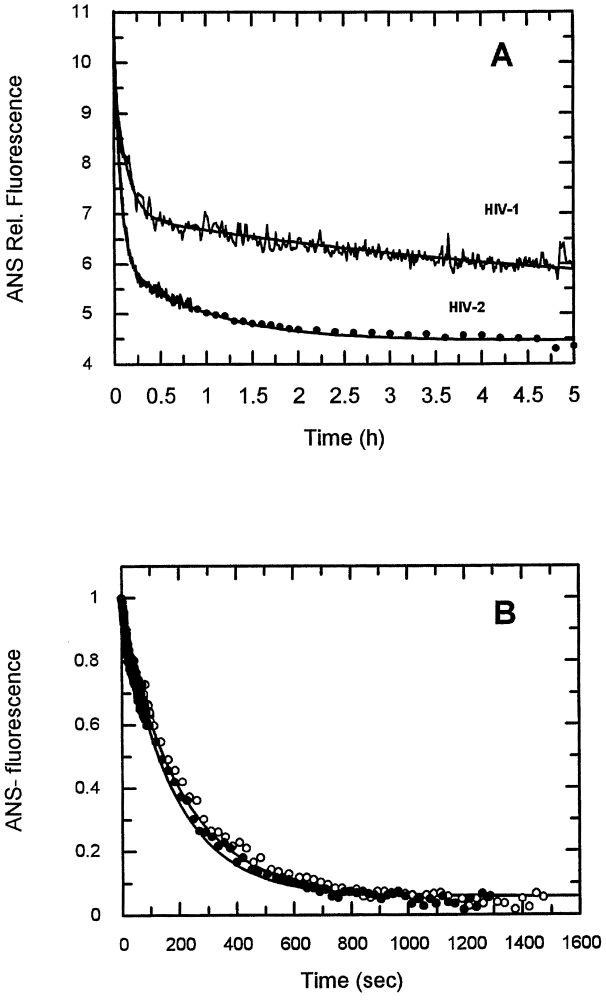

Figure 3. Time course of RT-dimerization monitored by ANS-fluorescence. RT (5 μM) was first dissociated using 20% acetonitrile and the dimerization was initiated by a 12-fold dilution in an acetonitrile-free buffer containing 2 μM ANS. The excitation was performed at 290 nm and the fluorescence resonance energy transfer occurring between the Trp residues and the probe (ANS) was monitored at 490 nm. The curves were fitted according to the sum of two exponential terms. A, The complete time course of the kinetic for both enzymes; B, corresponds to the normalized first phase fitted as a second order reaction.

provides a good signal for following either the RT dissociation or the monomer association in a time-dependent manner. The quenching of ANS-fluorescence upon RT dimerization can be directly correlated to the decrease in the accessible hydrophobic region of RT. The experiments were performed either by adding the probe in the dimerization buffer or using ANS previously bound to RT during the dissociation step. The concentrations used were 0.5 μM for RT and 2 μM for ANS. The ANS fluorescence due to fluorescence energy transfer between the Trp residues and ANS was used as a signal, measured at 490 nm upon excitation at 290 nm. As shown in Figure 3, the ANS-fluorescence decreased dramatically during RT-dimerization. At the end point of the curve the ANS-fluorescence was

~threefold higher than that of free ANS in solution, which is similar to the value obtained by monitoring the binding of ANS to native heterodimeric RT (not shown). In all cases, the kinetics showed a biphasic pattern and the data could be well fitted as the sum of two exponential terms with an amplitude of ~1:1 for the fast and slow term of the kinetic, respectively. It should be noted that this is not strictly the correct mathematical form for the fit, since the first phase reflects a second order reaction. To obtain an estimate of the second order rate constant, the initial phase was fitted using the equation for a second order reaction and treating the start of the second phase as a straight line. This led to rate constants of $4.5 \times 10^4\ M^{-1}\ s^{-1}$ for HIV-2 and $3.9 \times 10^4\ M^{-1}\ s^{-1}$ for HIV-1, which are similar to the values obtained from monitoring the intrinsic protein fluorescence (Figure 1), suggesting that both signals monitor the same step, i.e. initial monomer association.

This initial rapid phase is concentration-dependent in the range 0.25 to 1 μM and can be fitted to a second order equation (Figure 3B). In contrast, the second step is not dependent on the enzyme concentration and is ~12-fold faster for HIV-2 RT. The rate constants obtained of 0.095 h^{-1} (HIV-1) and 1.21 h^{-1} (HIV-2) are consistent with the recovery of polymerase activity measurements. The biphasic change in ANS-fluorescence revealed that both steps involve hydrophobic interactions. The first step is probably due to the interactions between the two ''connection domains'', mainly controlled by the Trp-cluster. The second step probably involves other subdomains of RT.

Using bis-ANS (4 μM) as a probe, no change in the extrinsic fluorescence was observed after dilution in the dimerization buffer and only 5 to 10% of heterodimer-RT was recovered after one hour incubation as measured by size exclusion-HPLC. These results suggest that the interaction with the large number of aromatic rings in the bis-ANS interferes with the RT-dimerization. This is in agreement with our earlier results, where it was shown that hydrophobic peptides corresponding to the Trp-cluster can act as powerful dimerization inhibitors (Divita *et al*., 1994).

Kinetics of binding of fluorescently labelled P/T

Fluorescently labelled primer/templates have been used as tools to investigate the kinetics of interaction of RT with its substrates (Müller *et al*., 1991*b*; Divita *et al*., 1993*b*). Here the binding of a fluorescently labelled primer/template during the RT-association was used to determine directly the rate of formation of a heterodimeric RT. The primer/template used is a 18/36-mer labelled on the last but one base at the 3'-end of the primer with a mansyl group. The fluorescence of the mansyl group offers the advantage of being extremely sensitive to variations in its environment. The binding of the primer/template to HIV-1 and HIV-2 RT induced a marked increase (~fourfold) of the mansyl-fluorescence and a 25 nm blue shift of the emission spectrum from 460 nm to 435 nm. As shown in Figure 4, the binding titration curve of the fluorescent primer/template to both RTs are monophasic and the evaluation of the data leads to a value of 3.4 nM (HIV-2 RT) and 4.0 nM (HIV-1 RT) for the dissociation constant by using fluorescence energy transfer between the Trp residues and the mansyl group as a signal. In contrast, it was shown that the primer/template did not bind to the monomeric forms of either enzyme. The titration of the intermediate dimeric form of RT (corresponding to HIV-1 RT dissociated by acetonitrile and fully reassociated by 40 minutes incubation in a free acetonitrile buffer) with the fluorescent primer/template is also monophasic. In this case a maximal fluorescence enhancement of threefold and a dissociation constant of 8.2 nM was obtained.

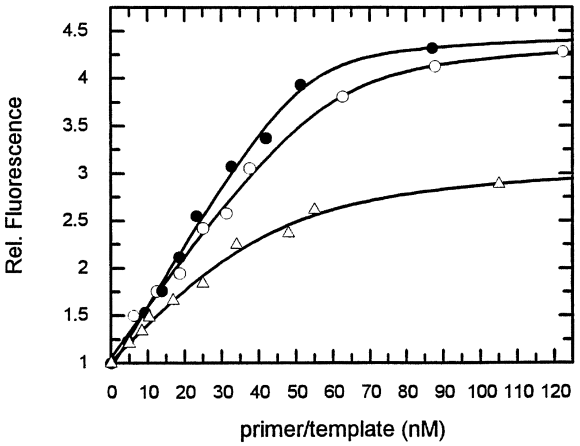

Figure 4. Binding of a mansyl-labelled primer/template to HIV RT. A fixed concentration of 50 nM HIV-1 RT (○), HIV-2 RT (●) or intermediate dimeric form of HIV-1 RT (△) (corresponding to dissociated RT, which have been fully reassociated by 40 minutes incubation in the dimerization buffer) was used and the titration was performed by increasing the concentration of fluorescent primer/template. The increase of the fluorescence of the mansyl group attached to the primer/template was monitored at 450 nm upon excitation at 290 nm. The data were corrected and analysed using a quadratic equation as described in Materials and Methods.

The dimerization experiments were performed by adding the primer/template (0.5 μM) in the association buffer, and measuring the fluorescence resonance energy transfer between the Trp residues and the mansyl-group at 450 nm (excitation at 290 nm). The time dependence of primer/template binding to HIV-1 and HIV-2 RT during the dimerization process was biphasic (Figure 5A and B). A total fluorescence increase of 3.6-fold was observed with amplitudes of 1/0.6 (fast/slow) for HIV-1 RT. The curve could be fitted well as the sum of two exponential terms: a fast first phase with a half life value of 2.8 minutes and 5.2 minutes and a second slow one with a rate constant of 0.22 h^{-1} and 0.09 h^{-1}

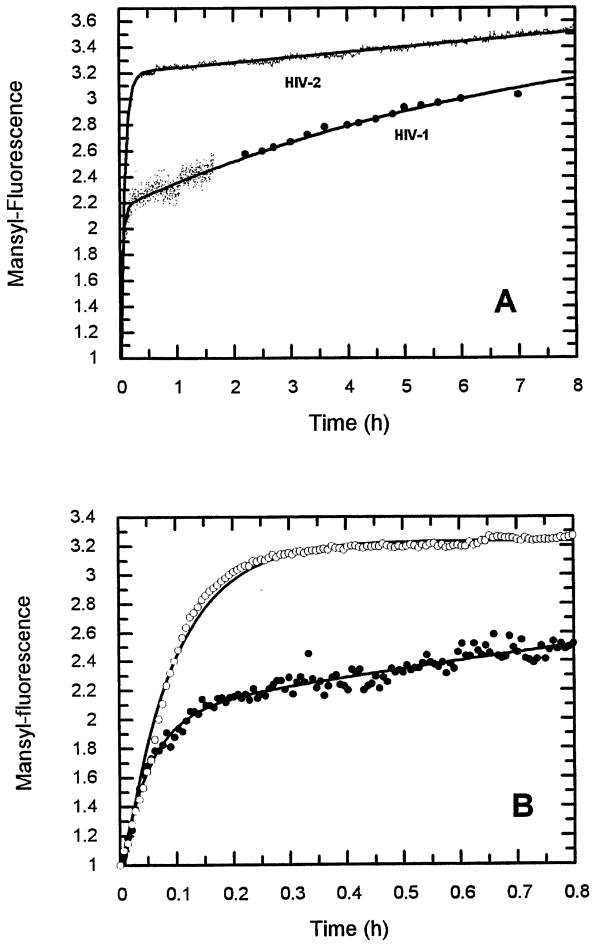

Figure 5. Time course of HIV-1 and HIV-2 RT dimerization monitored by the fluorescence of a mansyl-labelled primer/template. Mansyl-labelled primer/template was added in the association buffer (0.5 μM) and the kinetics of binding was monitored by measuring the fluorescence resonance energy transfer occurring between the Trp residues and the mansyl-group. The concentration of both RTs used was 0.45 μM. The excitation was performed at 290 nm and emission measured at 450 nm. The complete time course of the curves were fitted as a double exponential reaction (A). B, corresponds to the first phase of the HIV-1 (●) and HIV-2 RT (○) fitted as a second order reaction.

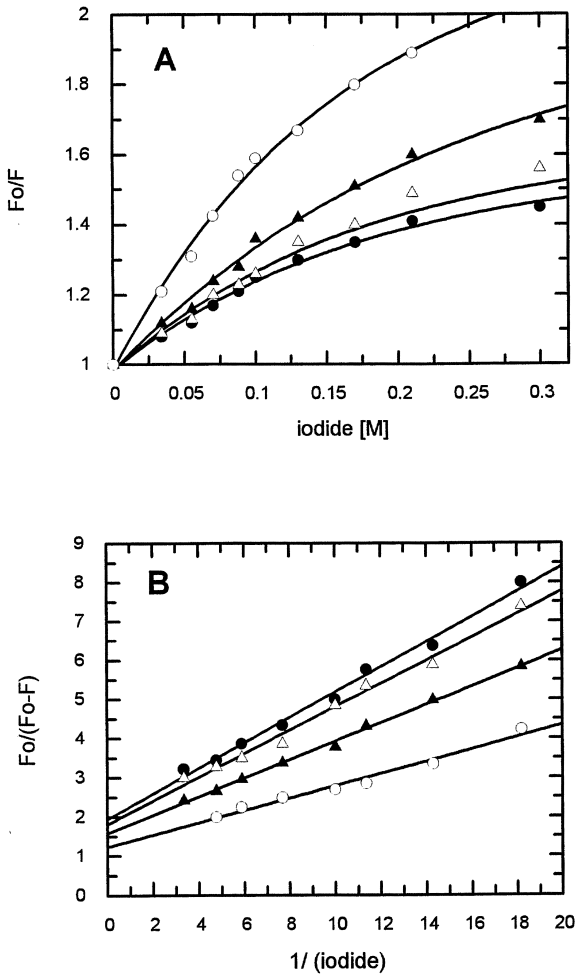

Figure 6. Stern-Volmer plots of iodide quenching at different times during the RT-dimerization. The iodide quenching experiments were performed using a concentration range of iodide between 0 and 0.3 M, on a sample fraction of a 0.5 μM RT-solution after 0 (○), 1 hour (●), 20 hours (△) of incubation in the dimerization buffer. As control the same experiment was performed on the native heterodimeric form of RT (●). The data were analysed according to the Stern-Volmer equation (A) and to the modified Lehrer equation (B).

for HIV-1 RT and HIV-2 RT, respectively. Fitting the first step as a second order reaction gives a similar rate constant to that already obtained for this phase using other methods (4.2×10^4 M^{-1} s^{-1}). As previously observed with ANS-fluorescence and Trp-fluorescence, the first phase is concentration-dependent.

These results demonstrate that the primer/template can bind to the inactive dimeric form and increase the rate of association by a factor of ~ 2. The presence of primer/template also increased the rate of the second phase by a factor 3 for HIV-1 RT. In the case of HIV-2 RT, this makes correct fitting of the second step difficult.

Modification of the Trp accessibility during the dimerization process

Iodide quenching experiments were used to characterize the accessibility of Trp residues to the solvent at different stages of the dimerization process. Iodide is a polar anionic quencher, which only has accessibility to the surface of folded proteins (Eftink & Ghiron, 1981; Eftink, 1991). The Stern-Volmer and modified Stern-Volmer plots are shown in Figure 6A and B. Native heterodimeric forms of RTs showed a limited accessibility to iodide with an extraolated Stern Volmer (K_{SV}) constant of 2.4 M^{-1}. Moreover, the Stern-Volmer plot presented a marked downward deviation from linearity due to a large fluorophore heterogeneity towards iodide, with an accessible fraction, f_a, of 0.5. In contrast, the dissociation of RT into its subunits strongly

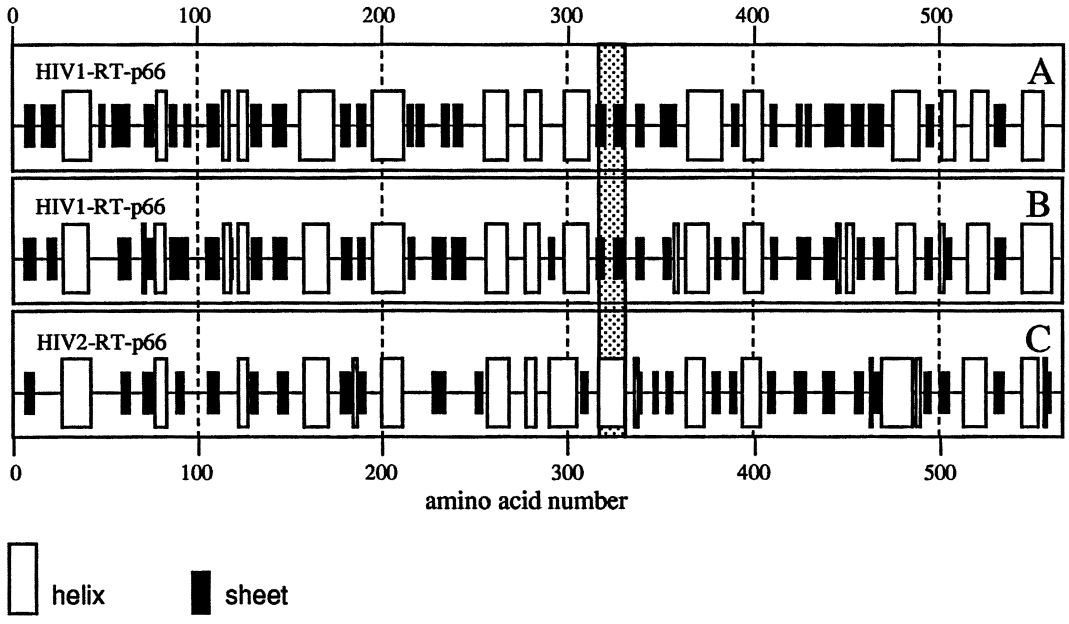

Figure 7. HIV-1 and HIV-2 RT secondary structure prediction using SOPM. A, The HIV-1 RT p66 subunit structure as obtained from X-ray data (Jacobo-Molina *et al*., 1993). B and C, The predicted secondary structures of HIV-1 RT and HIV-2 RT p66 subunits, respectively. Open and closed boxes correspond to the α-helices and β-strands, respectively. The main difference between the 2 enzymes is located in the amino acid sequence 312 to 340 and is marked by the broken box.

increased the accessibility to iodide with a corresponding Stern-Volmer constant of 5.2 M^{-1} and an accessible fraction of 0.8. Similar results were obtained for both HIV-1 and HIV-2 RTs. During RT dimerization, the quenching experiments were performed at defined time intervals (0, 1 and 20 hours) on samples of a RT-stock solution of 0.5 μM, using a range of iodide concentration from 0 to 0.3 M (Figure 6A and B). In all cases, the Stern-Volmer plots showed marked curvature (Figure 6A). The first step of the dimerization process (after one hour) is accompanied by a large decrease in the Trp-accessibility (K_{sv} = 3.2 M^{-1}) and increase of the Trp-heterogeneity (f_a = 0.6). In contrast, during the second phase only a small decrease in accessibility was observed, (K_{sv} = 2.6 M^{-1}) with a value that is not significantly different from that obtained for the native RTs.

HIV-2 RT secondary structure prediction

The kinetics of RT-dimerization obtained using different complementary approaches can be explained on the basis of a two step mechanism. The first relatively rapid step is concentration-dependent and corresponds to initial monomer association. The second phase is not dependent on the enzyme concentration and results in a change in the preformed dimer structure. This conformational reorganisation is required for the formation of active forms of the heterodimers and is ~12-fold faster for HIV-2 than for the HIV-1 enzyme. According to this, the protein domains involved in this conformational change should be significantly different between the two enzymes.

The two RTs (HIV-1_{BH10} and HIV-2_{D194}) show 60% identity in the amino acid sequence. In contrast to the structure of HIV-1 RT, which has been solved by X-ray crystallography to relatively high resolution (Kohlstaedt *et al*., 1992; Jacobo-Molina *et al*., 1993), no information is available on the structure of HIV-2 RT. For this reason the secondary structure prediction of HIV-2 RT was carried out using the self optimized prediction method (SOPM). In order to check this method, the HIV-1RT structure was predicted and compared to the X-ray deduced secondary structure. The prediction fits well with the crystallographic data (Figure 7 lanes A and B, observed and predicted, respectively) with an agreement level of 85%. Moreover, all the stretches of secondary structure have been properly located, the mispredicted amino acids being at the edges of the regular secondary structures. This comparison demonstrates the validity of the SOPM approach on these proteins. Thus, the secondary structure of HIV-2 RT has been predicted (Figure 7 lane C) and compared to that of HIV-1 RT. Although there are some rare regions with poor homology between both sequences, there is only a single segment, corresponding to positions 312 to 330, which is predicted to have different secondary structures. An α-helix is predicted in HIV-2 whereas two β-sheets are predicted and observed in HIV-1 RT. The primary sequence of this region shows less than 20% identity between the two RTs and the motif QEEEELE at positions 320 to 326 in the HIV-2_{D194} isolate is highly specific for HIV-2 RT. Because of the absence of homologous proteins in the protein data

bank (PDB), we have searched both for local similarities of this region 312 to 330 using FASTA (Lipman & Pearson, 1985) and for a pattern derived from multiple alignments of the HIV-2 family. Although the similarity levels are rather low, the hits obtained are mainly located in an α-helix, as in the case of the structure of triacylglycerol lipase (amino acids 110 to 126), chaperone protein papD (amino acids 160 to 175) and arabinose binding protein (amino acids 86 to 102). According to the nomenclature of Kohlstaedt *et al*. (1992), the region from 310 to 340 corresponds to β-sheet 15 of the thumb domain and the β-sheets 16 and 17 of the connection domain in the HIV-1 enzyme. This forms the junction between the two subdomains and seems to be involved as well in the interaction between the two subunits (p51 thumb and p66 RNAse-H domain) as in the primer / template binding site (p66 thumb domain).

Discussion

It is clearly established that the heterodimeric (p66 / p51) organisation of HIV-1 and HIV-2 RTs is absolutely required for the biological activity of RT. As we have proposed, the RT-dimerization constitutes an interesting target for a new antiviral therapy (Restle *et al*., 1990; Divita *et al*., 1994). A detailed knowledge of this process is essential for the design of new inhibitors. In the present work we have used different complementary approaches including fluorescence spectroscopy, size exclusion-HPLC and a polymerase activity assay to obtain a better understanding of the dimerization processes of HIV-1 and HIV-2 RT. The results for both enzymes can be described by a two step mechanism as proposed in the following minimal RT-dimerization pathway model:

Scheme 1

$$\text{p66} + \text{p51} \underset{k_{-1}}{\overset{k_1}{\Leftrightarrow}} \text{p66/p51} \underset{k_{-2}}{\overset{k_2}{\Leftrightarrow}} \text{p66/p51*}$$

The first step leads to a folded heterodimer intermediate (p66 / p51) devoid of enzymatic activity, which slowly isomerises to the mature heterodimeric form of RT (p66 / p51*). This slow isomerization is the rate-limiting step in the generation of the active form of the enzyme.

Both HIV-1 and HIV-2 RT were reversibly dissociated by treatment with acetonitrile to yield folded monomers without inducing denaturation (Restle *et al*., 1990; Divita *et al*., 1993*a*). This method offers the possibility of directly investigating the dimerization process and rapidly testing potential dimerization inhibitors. Such a controlled dissociation reduces the problem of aggregation, which may adversely affect the final yield of native oligomeric proteins, a problem encountered using denaturing methods (Jaenicke & Rudolph, 1986; Jaenicke, 1987).

Monomer association step

The first step of the dimerization process corresponds to the monomer-association. This bimolecular reaction is dependent on the protein concentration and follows a second order reaction with an association rate constant (k_1) which is similar for both HIV-1 and HIV-2 RTs in the range of 2×10^4 to 5×10^4 M^{-1} s^{-1}. This association step induces a dramatic change in the monomer structure as revealed by the change in intrinsic fluorescence. The large quenching of intrinsic fluorescence (25%) and the fact that 30% of the fluorophores are no longer accessible to iodide after monomer association suggests that many Trp residues are involved in this interaction. This is in good agreement with our earlier findings using connection domain-derived peptides as inhibitors (Divita *et al*., 1994) or mapping the subunit interface using monoclonal antibodies (Restle *et al*., 1992*b*), indicating that the Trp-cluster of the ''connection domain'' plays a key role in the dimerization process. For HIV-RT, as observed for numerous proteins (Janin & Chothia, 1990), it seems clear that the protein–protein interaction involves many aromatic residues. The decrease of the accessibility of the Trp residues towards iodide (40%) and the blue shift of the fluorescence emission spectrum (from 345 nm to 338 nm) indicates that the conformational change is associated with a reduction of the solvent-exposed hydrophobic domains of the monomers. The implication of hydrophobic regions of the protein in the dimerization is also reflected by the decrease in the ANS fluorescence.

The Trp-cluster of the connection domains located in the region of residues 389 to 414 (HIV-1 RT_{BH10}) contains a total of six Trp residues, which are highly conserved in the different clones of HIV-1 and HIV-2 RTs. Our results lead to the conclusion that the α-helix L and β-sheet 20 of the connection domain which contain this Trp-cluster are directly implied in the first step of the dimerization. This Trp-cluster has also been proposed to participate in protein–protein interactions by other authors (Baillon *et al*., 1991; Beccera *et al*., 1991; Restle *et al*., 1992*b*). Moreover, the recent studies of Jacques *et al*. (1994) based on a C-terminally truncated p51 subunit suggest that the folded structure of β-sheet 20 is required for dimer formation. Monitoring the dimer formation by size exclusion-HPLC shows that the monomer association corresponds to the large change in intrinsic fluorescence and is completely finished after one hour. The intermediate dimeric form of both RTs is devoid of polymerase activity, but can bind primer / template, albeit somewhat more weakly. It seems likely that the difference in stability between the homo- and heterodimer forms of RT (Restle *et al*., 1990) is associated with the conformational change occurring in the second step.

The large increase in the fluorescence of a mansyl labelled primer / template ($\sim$fourfold) upon binding to RT provides a sensitive tool for the study of dimerization kinetics. This kind of modified oligonucleotide has already been used to character-

ize DNA interaction with the Klenow fragment of *E. coli* DNA polymerase I (Allen *et al*., 1989; Allen & Benkovic, 1989). The dissociation constants of RTs for the fluorescently labelled primer/template (in the range of 3.5 to 4 nM) are quite similar to those observed for non-fluorescent primer/templates (Divita *et al*., 1993*b*), which suggests that the attached probe does not significantly modify the interaction with RT. The relatively low K_d (8.5 nM) for the complex between primer/template and the HIV-1 RT intermediate form implies that the primer/template binding site is well folded in this intermediate. The presence of the primer/template binding site in the intermediate form is not surprising and could be explained by the fact that this site is in part located at the subunit interface. In the crystal structure of HIV-1 RT complexed with a double-stranded DNA at 3.0 Å resolution (Jacobo-Molina *et al*., 1993), the primer/template binds in a large cleft formed by the fingers, palm and thumb subdomains of the p66 subunit, which is supported by the connection domains of p66 and p51 and by the thumb domain of p51 forming the floor of the cleft.

Maturation step

The absence of polymerase activity in the intermediate dimer implies that the correct organization of the catalytic site is not yet achieved at this stage and that a further conformational change is required for maturation to the fully active form of RT. The second step, corresponding to the recovery of the enzymatic activity of HIV-1 and HIV-2 RT, which represents the final stage of the RT-heterodimer maturation, occurs in a slow isomerization reaction, with a first order rate constant k_2 in the range of 0.1 to 0.2 h^{-1} for HIV-1 RT. This slow isomerization constitutes the rate-limiting step of the native RT formation process at micromolar RT concentrations. The kinetics of the biphasic change observed in the fluorescence of mansyl labelled primer/template or in the fluorescence of ANS upon RT dimerization showed that the rate of the second phase is not dependent on the enzyme concentration and takes place after the initial subunit association, which fits well with the kinetics of RT activity recovery. The decrease in ANS fluorescence during this second step to a value similar to that obtained for ANS-binding to the native RT, and in the Trp-accessibility towards iodide, suggests that the change in the intermediate-dimer structure involves hydrophobic interactions, just as the initial monomer association does. Moreover this conformational change appears to take place in the close environment of the polymerase catalytic site, as revealed by the increase in the fluorescence of the mansyl-labelled primer/template. The mansyl group attached to the last but one base of the primer is a powerful probe for monitoring the conformational evolution of the catalytic site. According to the structure of the HIV-1 RT polymerase active site, the fluorescent group would be close to the Trp residue at position 229 located at the end part of β-sheet 12. The β-hairpin formed by the strands β12 and β13 of the p66 subunit maintains the terminal primer nucleotide in the polymerase catalytic site (Jacobo-Molina *et al*., 1993). This close proximity would also be one of the reasons for the large fluorescence energy transfer observed between Trp residues and the mansyl-group upon primer/template binding to RT.

In contrast to the initial monomer association, which is of similar rate for HIV-1 and HIV-2 RT, the subsequent intermediate conformational change is faster for HIV-2 RT ($\sim$12-fold). The fluorescence and polymerase kinetic results demonstrate that the regions of the protein involved in this maturation step are significantly different between HIV-1 and HIV-2 RT and the interaction appears to be stronger in the HIV-2 enzyme. This difference agrees well with the higher stability of the HIV-2 heterodimer compared to HIV-1 (Müller *et al*., 1991*a*; Restle *et al*., 1992*b*) and the hypothesis that it is the conformational change of the intermediate which controls the stability of the different forms of RT.

A more detailed molecular interpretation of the dimer organization is based in part on the X-ray structure of the HIV-1 RT (Kohlstaedt *et al*., 1992; Jacobo-Molina *et al*., 1993) and on the prediction of the secondary structure of HIV-2 RT. The predicted HIV-2 RT secondary structure and its comparison with the HIV-1 RT structure were helpful for the identification of the domains involved in the two steps and for understanding the RT maturation process. The prediction of the secondary structure of HIV-2 RT was performed using the method SOPM described by Geourjon & Deleage (1994). This method has been tested on a large set of proteins where it has proved to be one of the most accurate. An accuracy of 85% was found between the predicted (this work) and the X-ray structure of HIV-1 RT (Jacobo-Molina *et al*., 1993). A comparison between the HIV-1 and HIV-2 RT secondary structure reveals only one major difference located in the region 312 to 332, corresponding to the end part of the thumb domain and the beginning of the connection domain. This region is predicted as an α-helix in HIV-2, instead of two β-sheets (β15 and β16) in HIV-1 RT. The HIV-2 RT sequences in this area reveal an homologous cluster of negative charges (321 to 326) with the glutamic acid motif EE(E-K)ELE, which is not present in HIV-1 RT. Such a motif has been found in a few other proteins of solved X-ray structure, such as triacylglycerol lipase (1TGL), the chaperone protein papD (3DPA) and arabinose binding protein (1ABP). In all cases, this motif is folded as an α-helix, which is not surprising, since an α-helix would be the most appropriate structure to keep apart the negative charges of the glutamic acids. This structural difference supports the idea of an important role of the thumb domain in the last stage of the organization of the mature RT and could be one of the explanations for the higher affinity of primer/templates to HIV-2 RT (Rittinger *et al*., unpublished results).

The thumb domain of the p66 subunit is involved

in the primer / template interaction with RT, as shown by the mapping of the binding site (Sobol *et al*., 1991; Basu *et al*., 1992) and by the X-ray structure (Jacobo-Molina *et al*., 1993). This subdomain is involved in the stabilization of the primer / template in the binding site and probably in its translocation during polymerization. In the present work, based on combining structure prediction and kinetic studies we suggest that the thumb domain is also involved in the folding and the organization of the native heterodimeric RT.

In the structure of HIV-1 RT, the dimer interface is mainly formed by the interaction between the two connection subdomains. Two other interactions were noted: between the thumb and connection domain of p51 and the RNase H domain of p66, and between the p51 fingers and the p66 palm and connection domains. The interaction resulting in the stacking of the p51 thumb domain to the p66 RNase H domain seems to be the key to the maturation and the stability of the heterodimeric form of both RTs. It should be present only in the heterodimeric form, absent in the p51 homodimer containing no RNase H domain and probably different in the p66 homodimer, which contains two RNase H domains. The nature of the *in vivo* pathway of RT maturation is not yet clear, but may require as a first step formation of a p66 / p66 homodimer involving mainly the two connection domains, which is followed by a proteolytic processing of one RNase H domain by the HIV protease (Kohl *et al*., 1988). The latter requires an asymmetric form of the p66 / p66 homodimer, in which one of the RNase H domains is partially unfolded to reveal the site of cleavage (Lowe *et al*., 1988; Sharma *et al*., 1994). The p66 / p66 dimerization could provide some of the energy required for the unfolding step, which seems to be the rate-limiting step for the processing of p66 / p66 (for a review see Jacobo-Molina & Arnold, 1991). After this, the interaction of the p51 thumb domain with the p66 RNase H domain takes place to give mature heterodimeric RTs. This is also supported by the fact that the main difference between HIV-1 and HIV-2 RT is located at the base of the thumb domain, which could control the mobility of this subdomain. Another part of the thumb domain has also been proposed to be involved in the dimer interface, which corresponds to the loop between the α-helix I and α-helix J containing a pseudo leucine zipper motif located in this position (Baillon *et al*., 1991; Goel *et al*., 1993). In the X-ray structure this loop is in close contact with the RNase H domain of the p66 subunit.

The second contact between the p51 and the p66 subunits involves the β-hairpin formed by the strands β-7 and β-8 of the p51 fingers domain, which is in close contact with the polymerase active site of p66. This region is located in the binding pocket of the non-nucleoside inhibitors (Smerdon *et al*., 1994). The structural reorganization of this region of the p51 fingers domain close to the catalytic site would be one of the events required for the polymerase activity, which appears during the isomerization step.

Based on these results we can conclude that a working model for the formation of heterodimeric RT from its subunits *in vitro* involves first the interaction of the central connection subdomains of the two subunits, followed by a conformational change which involves the two extreme parts of p51: the stacking of the thumb domain to the RNase H domain of p66 and the placement of the finger domain in the palm domain of p66. It is possible that this is not a direct reflection of events occurring during production of the mature form of RT *in vivo*. RT is produced on proteolytic processing of the 160 kDa gag-pol polyprotein by the viral protease, which is also part of the precursor protein. However, it is not known definitively at the present time what the order of events (i.e. of the various cleavage and multimerization processes) *in vivo* is. In spite of this, it is highly likely that the events seen on association of the monomeric components of the mature protein are analogous to or related to events that occur in *in vivo* processing, which will necessarily be more difficult to study. Extension of the present work to a study of dimerization and proteolysis of isolated p66 subunits is a first step in this direction, but even here the relevance to the situation *in vivo* must be considered critically, since studies with the full length polyprotein and with truncated versions of it indicate that dimerization or multimerization of the polyprotein can occur *via* any of the three enzymatically active proteins present (i.e. protease, RT or integrase; Gautel & Goody, unpublished; Gautel, 1990).

In addition to its relevance to the situation *in vivo*, examination of the dimerization mechanism of the RT heterodimer is of fundamental interest as a problem in protein folding. It also leads to ideas on potential ways of preventing or reversing dimerization, which could be of interest for chemotherapy of AIDS. We have recently shown that peptides derived from the connection domains are powerful inhibitors of monomer association (Divita *et al*., 1994). The results presented here lead to an extension to this approach, which involves targeting the second step of this process, the maturation.

Materials and Methods

Materials

ANS, Bis-ANS and mansylchloride were purchased from Molecular Probes Inc., acetonitrile (gradient grade) and potassium iodide were from Merck (Darmstadt, Germany). [^{3}H]dTTP was obtained from Amersham. All buffers were filtered and degassed before use.

Enzyme preparation

Recombinant HIV-1_{BH10} and HIV-2_{D194} reverse transcriptases were expressed in *Escherichia coli* and purified as described previously (Müller *et al*., 1989, 1991*a*). Highly homogeneous preparations of the heterodimeric forms of the enzyme resulting from co-expression of the 66 kDa and 51 kDa subunits (68 kDa and 54 kDa for HIV-2 RT, respectively) were used. In spite of this difference in molecular weights, we still refer to p66 and p51 subunits

for the HIV-2 RT in analogy to the nomenclature of the related polypeptides from HIV-1 RT. Enzyme concentrations were routinely determined as described by Bradford (1976) using a gravimetrically prepared solution of RT as standard.

Oligonucleotides

Oligodeoxynucleotides were synthesized on an Applied Biosystems 380 B DNA synthesizer and purified in two steps by HPLC reverse-phase chromatography on a Hypersil C18 column. First, a linear gradient from 15% to 35% acetonitrile in 0.1 M TEAA was used, and after removal of the dimethoxytrityl protecting group, oligonucleotides were further purified with a linear gradient of 7% to 14% acetonitrile in 0.1 M TEAA. Primer and template oligodeoxynucleotides were annealed by heating an equimolar mixture of both in 20 mM Tris-HCl (pH 7.5) for 15 minutes at 70°C, followed by cooling to room temperature over a period of two hours in a water bath. Routinely, an 18/36-mer oligonucleotide primer/template was used with the nucleotide sequence $^{5'}$-TCCCT-GTTCGGGCGCCAC-$^{3'}$ for the primer strand and $^{5'}$-TGTG-GAAAATCTCTAGCAGTGGCGCCCGAACAGGGA-$^{3'}$ for the template strand, which corresponds to the sequence of the natural primer binding site (PBS) (Wain-Hobson *et al*., 1985).

Synthesis of a fluorescently labelled primer/template

The oligonucleotide was synthesized on an Applied Biosystems 380B DNA synthesizer. At the specified position a phthalimide-protected 5-(aminopropyl)-2'-deoxyuridine 3'(diisopropylcyano-ethylphosphoramidit) was incorporated. This analogue was prepared by the method of Gibson & Benkovic (1987) and the modified oligonucleotide was purified in two steps by reverse-phase HPLC as described above. For derivatization 50 nmol of oligonucleotide was dissolved in 0.5 ml of 0.2 M Na_2CO_3/$NaHCO_3$ (pH 10.0) and 50 μl of 120 mM mansylchloride in acetone was added. The solution was allowed to react for 12 hours in the dark at room temperature. Thereafter 50 μl of a freshly prepared solution of mansylchloride was added and the reaction was continued for a further 24 hours. The precipitate was removed by centrifugation and the supernatant was lyophilized. After dissolving in water the labelled oligonucleotide was purified by reverse-phase HPLC on a Hypersil C18 column using a linear gradient of acetonitrile in 0.1 M TEAA of 7 to 12% in 25 minutes and 12 to 78% in 28 minutes with a flow rate of 2 ml/minute. The product was identified by the simultaneous presence of absorbance of the oligonucleotide at 260 nm and of the mansyl-group at 340 nm. The nucleotide sequence of the primer/template used was $^{5'}$-TCCCTGTTCGGGCGCC***U***C-$^{3'}$ for the primer and $^{5'}$-TGTGGAAAATCTCATGCAGAGGCGCCC-GAACAGGGA-$^{3'}$ for the template (the location of the mansyl-labelled deoxyuridine is shown in italics).

Polymerase RT assay

Polymerase activity was measured in a standard reaction assay using poly(rA)·$(dT)_{15}$ as primer/template and containing 50 mM Tris-HCl (pH 8.0), 80 mM KCl, 8 mM $MgCl_2$, 1 mM dithiothreitol, 20 μM [^{3}H]dTTP and 50 to 100 ng enzyme (Restle *et al*., 1990). Reactions were incubated for ten minutes at 37°C and stopped by the addition of 2 ml of ice-cold 5% trichloroacetic acid. Acid-insoluble material was collected on nitrocellulose filters (Schleicher & Schuell BA85) and the radioactivity retained on the filter was measured by scintillation counting. The RT preparations used showed a specific activity of about 10,000 units/mg, where one unit of enzyme catalyses the incorporation of 1 nmol of [^{3}H]dTMP in ten minutes at 37°C into acid-insoluble material. The kinetics of formation of the native RT were monitored on samples containing 50 ng protein after defined incubation times; enzymatic activity was measured for five minutes at 37°C, the short time being chosen to limit the possibility of further activation by dimerization.

Size exclusion-HPLC

Chromatography was performed using two HPLC columns in series (Bio-Rad TSK-250 followed by Bio-Rad TSK-125; both 7.5×300 mm) as previously described (Restle *et al*., 1990). The samples, containing 5 to 10 μg protein, were applied and eluted with 200 mM potassium phosphate (pH 7.0) at a flow rate of 0.8 ml/minute.

RT dimerization kinetics

Complete dissociation of HIV-1 and HIV-2 heterodimeric RTs was achieved by 20 minute incubation in a buffer containing 50 mM Mes-HCl (pH 6.0), 10 mM $MgCl_2$, 50 mM KCl, 1 mM dithiothreitol and 20% acetonitrile. This treatment induced a complete loss of polymerase activity as monitored by the standard polymerase RT-assay method (Divita *et al*., 1993*a*). The association of the subunits was initiated by a 12-fold dilution of the sample in an acetonitrile-free buffer, containing 50 mM Tris-HCl (pH 8.0), 5 mM $MgCl_2$, 50 mM KCl, 1 mM dithiothreitol and 10% glycerol, resulting in a final concentration of 1.6% acetonitrile. All experiments were performed at 25°C with an enzyme concentration of 2 to 10 μM and 0.2 to 2 μM for dissociation and association kinetics, respectively. The establishment of the dimerization equilibrium was followed in a time-dependent manner using fluorescence methods, size exclusion-HPLC and by monitoring the polymerase activity of the enzyme.

Fluorescence experiments

Fluorescence measurements were performed at 25°C using a SLM Smart 8000 spectrofluorometer equipped with a PH-PC 9635 photomultiplier, using spectral bandpasses of 2 nm and 8 nm for excitation and emission, respectively. Measurements were corrected for wavelength dependence of the exciting light intensity by the use of the quantum counter Rhodamine B in the reference channel. The intrinsic fluorescence emission of the RTs was measured in a total volume of 0.7 ml of fluorescence buffer containing 50 mM Tris-HCl (pH 8.0), 10 mM $MgCl_2$, 50 mM KCl and 1 mM dithiothreitol. For the dimerization studies 10% glycerol was added to increase stability. To analyse the effect of magnesium, the same buffer without $MgCl_2$ was used and 1 mM EDTA was added to chelate Mg^{2+} traces. For the dimerization kinetics protein fluorescence was routinely excited at 290 nm and the emission was measured at the wavelength of greatest intensity change (340 nm). All data were corrected for background intensity of the buffer, for dilution effects and the Raman scattering contribution.

To monitor the binding of ANS or bis-ANS, the excitation was performed at 290 nm and the emission spectrum was integrated between 440 and 580 nm. RT dimerization

kinetic experiments were performed both with the probe added to the dissociation buffer or to the dimerization buffer. For each experiment the final concentration of the probe used was 5 μM and the emission fluorescence due to energy transfer between the Trp residues and the probe was monitored at 490 nm.

The fluorescence emission spectrum of mansyl labelled primer / template was integrated between 380 nm and 580 nm upon excitation at 340 nm. The titration of mansyl labelled primer / template binding to both HIV-1 and HIV-2 RTs was performed by measuring the increase of the fluorescence emission of the mansyl group at 430 nm, upon excitation of Trp residues at 290 nm (bandpasses set at 2 and 8 nm for excitation and emission, respectively). Steady state experiments were done at a temperature of 25°C by adding portions of mansyl labelled primer / template to solution containing a constant concentration of Rts of 50 nM. Data were analysed using a quadratic equation as previously described by Müller *et al*. (1991*b*). RT dimerization kinetics were followed by monitoring the increase of fluorescence of the mansyl labelled primer / template upon binding to heterodimeric RT. The fluorescent primer / template (1 μM) was added directly to the association buffer.

Fluorescence quenching by iodide

Titrations with potassium iodide were performed at 25°C by sequential addition of samples from a 6 M stock solution, up to 0.4 M final concentration. The potassium iodide stock solution contained 0.1 mM sodium thiosulphate to prevent I_3^- formation. Using NaCl, it was shown that ionic strengths up to 0.4 M did not significantly modify the fluorescence emission of RT. The protein concentration used was 0.45 μM and the data were corrected for dilution (less than 5%) and for the buffer blank. All values are the means of four separate experiments. The fluorescence quenching data were analysed according to the Stern-Volmer equation, which assumes that all quenching is collisional (no static quenching) (Eftink & Ghiron, 1981):

$$F_0 / F = 1 + K_{sv}[Q], \quad (1)$$

where F_0 and F are the fluorescence intensities in the absence or the presence of quencher, K_{sv} is the collisional Stern-Volmer constant, and $[Q]$ is the quencher concentration. The plot of F_0 / F *versus* $[Q]$ is linear for a homogeneous population of emitting fluorophores. In contrast, fluorophore heterogeneity leads to a downward deviation from linearity. Such behaviour can be evaluated quantitatively using the modified Stern-Volmer relationship as described by Lehrer (1971)

$$F_0 / (F_0 - F) = 1 / ([Q] \cdot f_a \cdot K_Q) + 1 / f_a, \quad (2)$$

where f_a is the fractional number of accessible fluorophores and K_Q their collisional constant. The plot of $F_0 / (F_0 - F)$ *versus* $1 / [Q]$ allows a graphical determination of f_a.

Data analysis

Dimerization data were transferred to a personal computer and evaluated using the program Grafit (Erithacus software), which allows the user to define his own equations. Kinetic simulations were performed with the program KinSim (N. Miller). The experimental data from the intrinsic fluorescence measurements were transformed to give the relative fraction of monomers. For each value of f_{obs} the monomeric fraction of RT (M_m) was calculated applying the following equation (Pace *et al*., 1990):

$$M_m = (f_{obs} - f_d) / (f_m - f_d), \quad (3)$$

where f_d and f_m are the fluorescence intensities of heterodimeric (obtained in the absence of dissociating agent) and monomeric RT (obtained at high concentration of dissociating agent), respectively.

Secondary structure prediction method

The secondary structure prediction method (Self-Optimised Prediction Method, SOPM) has been described by Geourjon & Deleage (1994). This method is composed of four main steps. The first one consists of the set up of a subset of proteins with known structure using extensive sequence comparisons. The second step is the submission of each protein sequence of the subset to a similarity-based prediction. The third step is an iterative optimisation of the prediction by the modification of the predictive parameters. The last step applies the optimised parameters to the query sequence. This method yields 69% predictive success on average and constitutes one of the most accurate methods yet available.

Acknowledgements

This work was supported by the Bundesministerium für Forschung und Technologie (BMFT). C.G. is a recipient of a fellowship from the Région Rhône-Alpes.

References

Allen, D. J. & Benkovic, S. J. (1989). Resonance energy transfer measurements between substrate binding sites within the large (Klenow) fragment of *Escherichia coli* DNA polymerase I. *Biochemistry*, **28**, 9586–9593.

Allen, D. J., Darke, P. L. & Benkovic, S. J. (1989). Fluorescent oligonucleotides and deoxynucleotide triphosphates: preparation and their interaction with the large (Klenow) fragment of *Escherichia coli* DNA polymerase I. *Biochemistry*, **28**, 4601–4607.

Baillon, J. G., Kumar, A., Wilson, S. H. & Jerina, D. M. (1991). A leucine zipper-like motif may mediate HIV reverse transcriptase subunit binding. *New Biologist*, **3**, 1015–1019.

Barré-Sinoussi, F., Chermann, J. C., Rey, F., Nugeyre, M. T., Chamaret, S., Gruest, J., Dauguet, C., Axler-Blin, C., Brun-Vezinet, F., Rouzioux, C., Rozembaum, W. & Montagnier, L. (1983). Isolation of a T-lymphotropic retrovirus from a patient at risk for acquired immunodeficiency syndrome (AIDS). *Science*, **220**, 868–871.

Basu, A., Ahluwalia, K. K., Basu, S. & Modak, M. J. (1992). Identification of the primer binding domain in human immunodeficiency virus reverse transcriptase. *Biochemistry*, **31**, 616–623.

Becerra, S. P., Kumar, A., Lewis, M. S., Widen, S. G., Abbotts, J., Karawya, E. M., Hughes, S. H., Shiloach, J. & Wilson, S. H. (1991). Protein–protein interactions of HIV-1 reverse transcriptase: implication of central and C-terminal regions in subunit binding. *Biochemistry*, **30**, 11707–11719.

Bradford, M. (1976). A rapid and sensitive method for the quantitation of microgram quantities of protein

utilizing the principle of protein-dye binding. *Anal. Biochem.* **72**, 248–254.

De Clercq, E. (1992). HIV inhibitors targeted at the reverse transcriptase. *AIDS Res. Hum. Retro.* **8**, 119–134.

Di Marzo Veronese, F., Copeland, T. D., De Vico, A. L., Rahman, R., Oroszlan, S., Gallo, R. C. & Sarngadharan, M. G. (1986). Characterization of highly immunogenic p66/p51 as the reverse transcriptase of HTLV-III/LAV. *Science*, **231**, 1289–1291.

Divita, G., Restle, T. & Goody, R. S. (1993*a*). Characterization of the dimerization process of HIV-1 reverse transcriptase heterodimer using intrinsic protein fluorescence. *FEBS Letters*, **324**, 153–158.

Divita, G., Müller, B., Immendörfer, U., Gautel, M., Rittinger, K., Restle, T. & Goody, R. S. (1993*b*). Kinetic of interaction of HIV reverse transcriptase with primer/template. *Biochemistry*, **32**, 7966–7971.

Divita, G., Restle, T., Goody, R. S., Chermann, J.-C. & Baillon, J. G. (1994). Inhibition of human immunodeficiency virus type 1 reverse transcriptase dimerization using synthetic peptides derived from the connection domain. *J. Biol. Chem.* **269**, 13080–13083.

Dobson, C. M., Evans, P. A. & Radford, S. E. (1994). Understanding how proteins fold: the lysozyme story so far. *Trends Biochem. Sci.* **19**, 31–37.

Eftink, M. R. (1991). Fluorescence techniques for studying protein structure. *Methods Biochem. Anal.* **35**, 127–205.

Eftink, M. R. (1994). The use of fluorescence methods to monitor unfolding transitions in proteins. *Biophys. J.* **66**, 482–501.

Eftink, M. R. & Ghiron, C. A. (1981). Fluorescence quenching studies with proteins. *Anal. Biochem.* **114**, 199–227.

Gautel, M. (1990). Dimerization der *gag-pol*- und *pol*-Polyproteine von HIV-1 und Aspekte der *pol*-Prozessierung in zellfreien Translationssystemen. M.D. Thesis, University of Heidelberg.

Geourjon, C. & Deleage, G. (1994). SOPM: a self-optimized method for protein secondary structure prediction. *Protein Eng.* **7**, 157–164.

Gibson, K. J. & Benkovic, S. J. (1987). Synthesis and application of derivatizable oligonucleotides. *Nucl. Acids Res.* **15**, 604–609.

Goel, R., Beard, W. A., Kumar, A., Casas-Finet, J. R., Strub, M. P., Stahl, S. J., Lewis, M. S., Bebenek, K., Becerra, S. P., Kunkel, T. A. & Wilson, S. A. (1993). Structure/function studies of HIV-1 reverse transcriptase: dimerization-defective mutant L289K. *Biochemistry*, **32**, 13012–13018.

Grob, P. M., Wu, J. C., Cohen, K. A., Ingraham, R. H., Shih, C. K., Hargrave, K. D., Mc. Tague, T. L. & Merluzzi, V. J. (1992). Nonnucleoside inhibitor of HIV-1 reverse transcriptase:nevirapine as a prototype drug. *AIDS Res. Hum. Retro.* **8**, 145–152.

Jacobo-Molina, A. & Arnold, E. (1991). HIV reverse transcriptase structure–function relationships. *Biochemistry*, **30**, 6351–6361.

Jacobo-Molina, A., Ding, J., Nanni, R. G., Clark, A. D. Jr, Lu, X., Tantillo, C., Williams, R. L., Kamer, G., Ferris, A. L., Clark, P., Hizi, A., Hughes, S. H. & Arnorld, E. (1993). Crystal structure of human immunodeficiency virus type 1 reverse transcriptase complexed with double-stranded DNA at 3.0 Å resolution shows bent DNA. *Proc. Nat. Acad. Sci., U.S.A.* **90**, 6320–6324.

Jacques, P. S., Wöhrl, B. M., Howard, K. J. & Le Grice, S. F. J. (1994). Modulation of HIV-1 reverse transcriptase function in ''selectively deleted'' p66/p51 heterodimers. *J. Biol. Chem.* **269**, 1388–1393.

Jaenicke, R. (1987). Folding and association of proteins. *Progr. Biophys. Mol. Biol.* **49**, 117–237.

Jaenicke, R. & Rudolph, R. (1986). Refolding and association of oligomeric proteins. *Methods Enzymol.* **131**, 218–250.

Janin, J. & Chothia, C. (1990). The structure of protein-protein recognition sites. *J. Biol. Chem.* **265**, 16027–16030.

Kohl, N. E., Emini, E. A., Schleif, W. A., Davis, L. J., Heimbach, J. C., Dixon, R. A. F., Scolnick, E. M. & Sigal, I. S. (1988). Active protease is required for viral infectivity. *Proc. Nat. Acad. Sci., U.S.A.* **85**, 4686–4690.

Kohlstaedt, L. A., Wang, J., Friedman, J. M., Rice, P. A. & Steitz, T. A. (1992). Crystal structure at 3.5 Å resolution of HIV-1 reverse transcriptase complexed with an inhibitor. *Science*, **256**, 1783–1790.

Lehrer, S. S. (1971). Solute perturbation of protein fluorescence. The quenching of the tryptophyl fluorescence of model compounds and of lysozyme by iodide ion. *Biochemistry*, **10**, 3254–3262.

Lightfoote, M. M., Coligan, J. E., Folks, T. M., Faucy, A. S., Martin, M. A. & Venkatesan, S. (1986). Structural characterization of reverse transcriptase and endonuclease polypeptides of the acquired immunodeficiency syndrome retrovirus. *J. Virol.* **60**, 771–775.

Lipman, D. J. & Pearson, W. R. (1985). Rapid and sensitive protein similarity searches. *Science*, **227**, 1435–1440.

Lowe, D. M., Aitken, A., Bradley, C., Darby, G. K., Larder, B. A., Powell, K. L., Purifoy, J. M., Tisdale, M. & Stammers, D. K. (1988). HIV-1 reverse transcriptase: crystallization and analysis of domain structure by limited proteolysis. *Biochemistry*, **27**, 1433–1436.

Müller, B., Restle, T., Weiss, S., Gautel, M., Sczakiel, G. & Goody, R. S. (1989). Co-expression of the subunits of the heterodimer of HIV-1 reverse transcriptase in *Escherichia coli*. *J. Biol. Chem.* **264**, 13975–13978.

Müller, B., Restle, T., Kühnel, H. & Goody, R. S. (1991*a*). Expression of the heterodimeric form of human immunodeficiency virus type 2 reverse transcriptase in *Escherichia coli* and characterization of the enzyme. *J. Biol. Chem.* **266**, 14709–14713.

Müller, B., Restle, T., Reinstein, J. & Goody, R. S. (1991*b*). Interaction of fluorescently labeled dideoxynucleotides with HIV-1 reverse transcriptase. *Biochemistry*, **30**, 3709–3715.

Nanni, R. G., Ding, J., Jacobo-Molina, A., Hughes, S. H. & Arnold, E. (1993). Review of HIV-1 reverse transcriptase three-dimensional structure: implications for drug design. *Perspect. Drug Discov. Design*, **1**, 129–150.

Pace, C. N., Shirley, B. A. & Thomson, J. A. (1990). Measuring the conformation stability of a protein. In *Protein Structure: A Practical Approach* (Creighton, T. E., ed.), pp. 311–330, IRL Press, Oxford, England.

Popovic, M., Sarngadharan, M. G., Read, E. & Gallo, R. C. (1984). Detection, isolation and continuous production of cytopathic retroviruses (HTLV-III) from patient with AIDS and pre-AIDs. *Science*, **224,** 497–500.

Ptitsyn, O. B. (1994). Kinetic and equilibrium intermediates in protein folding. *Protein Eng.* **7**, 593–596.

Ptitsyn, O. B., Pain, R. H., Semisotnov, G. V., Zerovnik, E. & Razgulyaev, O. I. (1990). Evidence for a molten globule state as a general intermediate in protein folding. *FEBS Letters*, **262**, 20–24.

Restle, T., Müller, B. & Goody, R. S. (1990). Dimerization of human immunodeficiency virus type 1 reverse transcriptase. *J. Biol. Chem.* **265**, 8986–8988.

Restle, T., Müller, B. & Goody, R. S. (1992*a*). RNAse-H activity of HIV reverse transcriptases is confined

exclusively to the dimeric forms. *FEBS Letters*, **300**, 97–100.

Restle, T., Pawlita, M., Sczakiel, G., Müller, B. & Goody, R. S. (1992*b*). Structure-function relationships of HIV-1 reverse transcriptase determinated using monoclonal antibodies. *J. Biol. Chem.* **267**, 14654–14661.

Sharma, S. K., Fan, N. & Evans, D. B. (1994). Human immunodeficiency virus type 1 (HIV-1) recombinant reverse transcriptase. Asymmetry in p66 subunits of the p66/p66 homodimer. *FEBS Letters*, **343**, 125–130.

Smerdon, S. J., Jäger, J., Wang, J., Kohlstaedt, L. A., Chirino, A. J., Friedman, J. M., Rice, P. A. & Steitz, T. A. (1994). Structure of the binding site for nonnucleoside inhibitors of the reverse transcriptase of human immunodeficiency virus type 1. *Proc. Nat. Acad. Sci., U.S.A.* **91**, 3911–3915.

Sobol, R. W., Suhadolnik, R. J., Kumar, A., Lee, B. J., Hatfield, D. L. & Wilson, S. H. (1991). Localization of a polynucleotide binding region in the HIV-1 reverse transcriptase: implication for primer binding. *Biochemistry*, **30**, 10623–10631.

Wain-Hobson, S., Sonigo, P., Danos, O., Cole, S. & Alizon, M. (1985). Nucleotide sequence of the AIDS virus, LAV. *Cell*, **40**, 9–17.

Edited by J. Karn

(Received 19 August 1994; accepted 25 October 1994)